Rule Set Transferability for Object-Based Feature Extraction: An Example for Cirque Mapping

Anders, N.S.; Seijmonsbergen, A.C.; Bouten, W.

DOI
10.14358/PERS.81.6.507

Publication date
2015

Document Version
Final published version

Published in
Photogrammetric Engineering and Remote Sensing

Rule Set Transferability for Object-Based Feature Extraction: An Example for Cirque Mapping

Niels S. Anders, Arie C. Seijmonsbergen, and Willem Bouten

Abstract

Cirques are complex landforms resulting from glacial erosion and can be used to estimate Equilibrium Line Altitudes and infer climate history. Automated extraction of cirques may help research on glacial geomorphology and climate change. Our objective was to test the transferability of an object-based rule set for the extraction of glacial cirques, using lidar data and color-infrared orthophotos. In Vorarlberg (W-Austria), we selected one training area with well-developed cirque components to parameterize segmentation and classification criteria. The rule set was applied to three test areas that are positioned in three altitudinal zones. Results indicate that the rule set was successful (81 percent) in the training area and a higher situated area (71 percent). Accuracy decreased in the two lower situated test areas (66 percent and 51 percent). We conclude that rule sets are transferable to areas with a comparable geomorphological history. Yet, significant deviation from the training area requires a different extraction strategy.

Introduction and Background

Cirques are complex landforms resulting from glacial erosion. Ivy-Ochs *et al.* (2008), regard a cirque as "a landform eroded by a glacier positioned in isolated niches in mountains." Three main cirque components are commonly recognized (see Plate 1): (a) an upper semi-circular "cirque divide" bounded by (b) steep surrounding slopes or "cirque headwall" and (c) a relatively flat lower surface or "cirque floor" bordering the headwall. In many cirques, three sub-components related to (de)glaciation are found on the cirque floor: (1) a 'cirque threshold' developed in bedrock, (2) (a) cirque moraine(s), representing recessional phases of the former cirque glacier, and (3) a "cirque lake" often located in the lowest part of the valley floor in between cirque moraines and cirque threshold. In certain areas (e.g., western Austria) cirque glaciers were active during the waxing and waning stages of former glaciations (De Graaff *et al.* 2007), their existence linked to former Equilibrium Line Altitudes (ELAs). The identification of cirques and cirque components can help in the reconstruction of former ELAs and contribute to studies concerning climate change.

Modern remote sensing data sets such as lidar (Light Detection and Ranging) elevation data, aerial photography and satellite imagery are powerful sources for the identification and analysis of (glacial) landforms such as cirques (Schneevoigt *et al.* 2008; Smith *et al.* 2006; Smith and Pain, 2009). Manual identification and digitization however can be time-consuming, especially when larger study areas are of interest. Geospatial Object-Based Image Analysis (GEOBIA) is a promising tool to analyze (glacial) landscapes (e.g., Saha *et al.*, 2011). With GEOBIA, image grid cells are clustered to form objects that can be classified based on internal grid cell values, shape characteristics, and topological relations. The clustering of grid cells makes GEOBIA particularly useful when used with high-resolution data sets. In this context, detailed morphometric characteristics of cirque components can be addressed in rule sets to (semi-) automatically map the distribution of cirques.

Transformation of conceptual semantic models for cirques into rule sets was emphasized by Eisank (2013) as a necessity to develop transparent workflows in order to improve objectivity and transferability of rule sets. This way, it is possible to further automate the creation of maps containing different landscape features (Drăguţ and Blaschke, 2006). Research on cirques that use a GEOBIA approach are scarce and generic rule sets for detection of cirques do not yet exist. Eisank *et al.* (2010) and Ardelean *et al.* (2011) both used mean curvature derived from digital elevation data for the segmentation of cirques, focusing on the upper divides. Altitudinal thresholds were used in combination with specific context rules as input for segmentation and classification. Altitudinal boundary conditions however, prevent the transferability of rule sets to other areas that are positioned higher or lower in the landscape than the training area. Anders (2013) has developed rule sets that can successfully extract (glacial) landforms in mountainous terrain from DEMs by using selected combinations of Land Surface Parameters (LSPs). By using multiple LSPs, classification rules may be formulated without altitudinal boundary conditions so that they are potentially transferable to other areas.

A possible concept that can be used to improve cirque classification is by taking into account the cirques degree of deviation from a "textbook example" or prototype landform (Evans, 2012), thus addressing a cirque's potential polygenetic history. This degree of deviation can result from a difference in length of the glaciation phase producing well or less developed cirques, or can be addressed to differences in the activity of post-glacial processes. Post-glacial landscape modification, for example fluvial erosion and accumulation may thus also disguise the boundaries of the main components of a cirque (Plate 1).

Our objective is to develop and test an object-based rule set that decomposes lidar DEMs into the three main cirque components: divide, cirque headwall, and cirque floor, and into the subcomponent cirque lake. The transferability of the rule sets will be evaluated for areas that are in different states of development. Our hypothesis is that rule sets to classify cirques can successfully be transferred to regions with a similar glacial and post-glacial history, but will perform less well in areas with a different geomorphological history. Based on the results found, this paper addresses a discussion on the transferability of GEOBIA rule sets in the extraction of geomorphological features from digital elevation data.

Niels S. Anders is with Soil Physics and Land Management, Wageningen University, P.O. Box 47, 6700 AA, Wageningen, The Netherlands (niels.anders@wur.nl).

Arie C. Seijmonsbergen and Willem Bouten are with the Institute for Biodiversity and Ecosystem Dynamics, Computational Geo-Ecology, University of Amsterdam, P.O. Box 94248, 1090 GE, The Netherlands.

Photogrammetric Engineering & Remote Sensing
Vol. 81, No. 6, June 2015, pp. 507–514.
0099-1112/15/507–514

doi: 10.14358/PERS.81.6.507

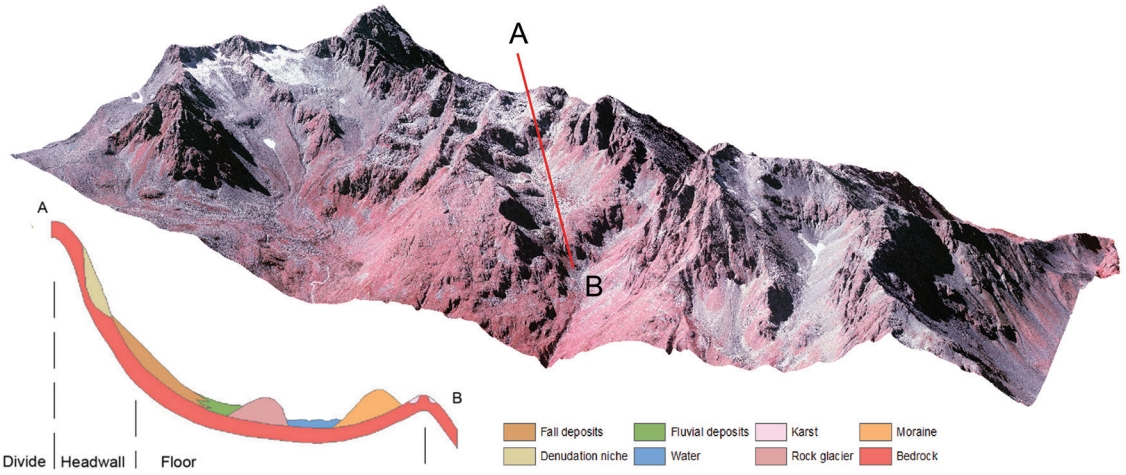

Plate 1. Perspective view of a color-infrared image of a cirque complex (Area 2, see Figure 1). The inset illustrates a hypothetical cross section of a cirque, including cirque components Divide, Headwall, and Floor, and the potential disguising of glacial components due to post-glacial landform development.

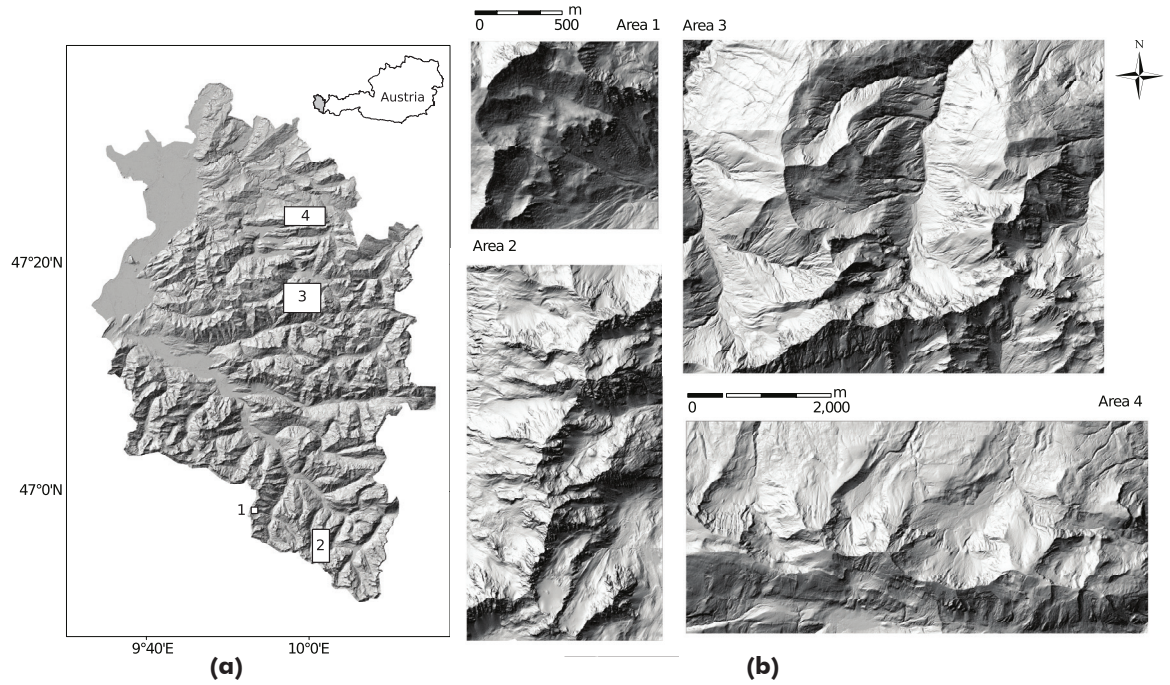

Figure 1. (a) The study area, located in the State of Vorarlberg, western Austria. The black rectangles show the location of the four test areas that are presented by lidar-derived shaded relief images in (b).

Study Area

Four clusters of cirques have been selected in the State of Vorarlberg, western Austria (Figure 1). In Vorarlberg, the glacier network developed in relation to the relative altitude of feeding areas during glaciations: higher areas became glaciated first, while lower areas became glaciated in later phases (De Graaff *et al.*, 2007). Moreover during early late-glacial phases, relatively low-lying cirques became ice-free while higher located cirques remained glaciated, a response to the rise in the ELA after climatic warming. For low-lying cirques this means that they have been glacially eroded for a shorter period of time. This may indicate that the resulting cirques including their (sub) components are potentially less developed and have been subject to denudation and accumulation processes, such as fluvial erosion and fall type mass movements, for longer. The selected four cirque clusters differ in altitude (see Table 1), and may therefore hold well to less developed cirque components which reflect increasing deviation from a "textbook example" of a cirque. This approach therefore substitutes altitude for time to represent differing states of cirque development.

Methods

We trained segmentation parameters and classification criteria of a relatively small area (Area 1: see Figure 1 and Table 1) for the extraction of the cirque divide, headwall, floor, and cirque lake. Subsequently, we tested the transferability of the rule set to the other three areas at different altitudinal zones. The training area is positioned relatively high and therefore had a relatively long period of glaciation which resulted in well-developed cirque components. Details of the training of the rule set and application to the test areas are further described in

Table 1. Subset Area Characteristics

Area nr	Area name	Mean elevation [m.a.s.l.]	Area size [km²]	Altitudinal zone
1	Gargellen-West	2285	1	+
2	Hochmäderer	2421	15	++
3	Zitterklapfen	1676	29	-
4	Winterstaude	1349	20	--

the *Training the Rule Set* Section. Classification metrics such as user's and producer's accuracy (Congalton, 1991) were used to quantify the performance of the rule set in the specific areas, see the *Validation of the Rule Set* Section for details.

The data sources consisted of (a) a lidar data set from 2011 from which the raw point data were acquired, filtered, and interpolated using linear squares interpolation into 1 m resolution lidar raster DTMs by TopScan (*http://www.TopScan.de/*); and (b) a Color Infrared (CIR) orthorecitified mosaic with 0.25 m resolution produced from aerial photographs acquired in 2001. The CIR data set is comprised of bands in the near-infrared (NIR), green and red light. Based on the lidar dataset several LSPs have been calculated using ArcGIS® 10.2 and python/GDAL: Shaded Relief, Slope Angle, Relative Elevation (REL, i.e., percentage of grid cells lower than a center grid cell in a given moving window), and Topographic Openness (Yokoyama *et al.*, 2002). The main steps of the analysis are based on the approaches of Anders *et al.* (2011).

The GEOBIA workflow is presented in Figure 2 and was carried out using eCognition® Developer 8.8. The numbers in the flow chart refer to processing steps which are explained in the following section.

Training the Rule Set

The Gargellen-West area was selected as training area because of the well-developed glacial features and the small size of the study area. Based on visual interpretation of the lidar LSPs and CIR imagery of the Gargellen-West area, three training samples per cirque component were manually digitized (Step 2 in Figure 2; see Plate 2). Only two training samples of cirque lakes were digitized due to the absence of more representative features in the area.

The training samples were used to calculate frequency distribution matrices of LSP values within the enclosed polygon boundaries (Anders *et al.* 2011; Anders, 2013, step 3 in Figure 2). The selection of LSPs used for the frequency distribution matrices was based on expert knowledge, so that unique properties of the three main components for this particular landform are captured. For cirque lake NIR values were used, as NIR images clearly show water bodies due to high absorption of the NIR light wavelengths. Slope Angle and Relative Elevation (measured within a 51 m × 51 m window) were used to create frequency distribution matrices of cirque divides, because divides are only found high in the landscape and landform units/elements are well separated by slope units. Slope Angle and Topographic Openness (measured within a 251 m × 251 m window) were used to create frequency distribution matrices of the cirque floor and headwall components, because both components can be differentiated by slope angle (relatively steep slopes at the cirque headwalls, and relatively gentle slopes on the cirque floors) and Topographic Openness clearly depicts boundaries between different landforms (Anders, 2013; Anders *et al.* 2013). The window sizes were manually selected to provide the required detail and texture for the scale of the landforms (i.e., Topographic Openness) or to provide the required regional information (i.e., Relative Elevation).

Subsequently, eCognition Developer (8.8) was used to create sets of image objects using the multi-resolution (MR) segmentation algorithm described by Baatz and Schäpe (2000). The MR segmentation algorithm is a region-growing procedure where neighboring grid cells and objects are merged (Baatz and Schäpe, 2000). The merging is rejected if the standard deviation of the objects before and after merging is higher than a given threshold. This threshold is set by a "scale" parameter. The theoretical range of scale parameter values is from 1 to infinity, where a value of 1 produces objects of one or few grid cells, and a large value results in the clustering of all grid cells into a single object. Due to the nature of the MR segmentation algorithm, the actual relation between the scale parameter value and object size depends on the spatial resolution and standard deviation of values in the data set. Multiple sets of image objects were created with different scale parameters (step 4 in Figure 2), which greatly affects the number of grid cells being clustered thus the size of individual objects. The sets of objects were created with scale parameter values of 10, 15, 20, 25, 30, 35, 40, 45, 50, 75, 100, 125, 150, 175, 200, 225, 250, 300, 500, and 999, respectively. This range was found large enough so that the optimal object size could be identified for each cirque component. The MR segmentation algorithm also requires the definition of a "shape" and

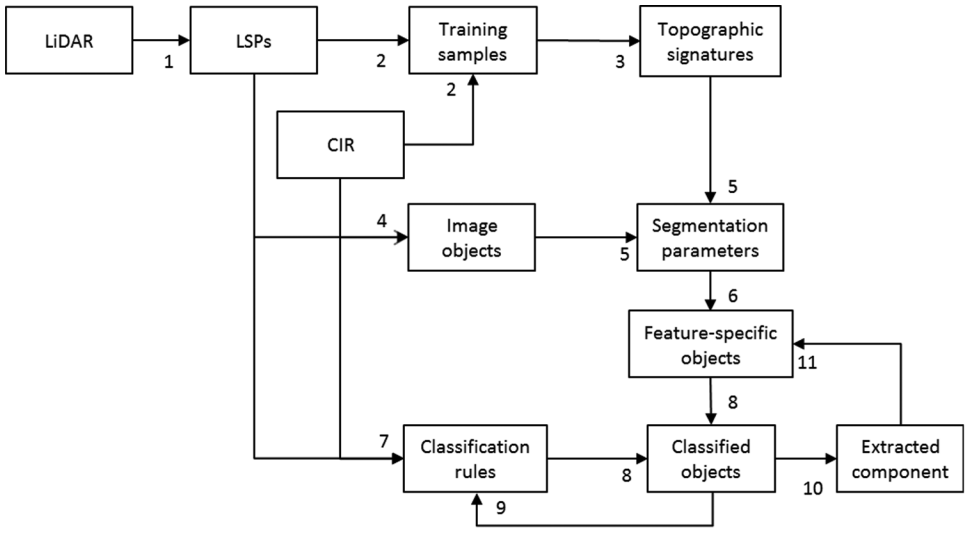

Figure 2. A schematic overview of the stratified GEOBIA workflow.

"compactness" parameter, which determine the degree of roundness and compactness the objects shape are forced into (ranging from 0 to 1), thus influences the geometry of objects. We manually selected a shape and compactness parameter value of 0.3 and 0.5, respectively, for all segmentations to prevent the generation of very irregularly shaped objects, but allowing objects to form primarily on the basis of the underlying raster data sets.

The frequency distribution matrices of the training samples were compared with the frequency distribution matrices of the overlapping image objects at five different point locations within each training sample. Based on the sum of absolute error between both matrices, a segmentation score is calculated. The average score out of five comparisons per training sample was used to evaluate segmentation accuracy of each set of objects and to determine an optimal scale parameter value (step 5 in Figure 2). Many segmentation evaluation methods exist with each their strengths and weaknesses to evaluate different kinds of segmentations of different kinds of data sets, and for different purposes (Zhang, 1996). The method used in this study can be justified by our goal to capture the same topographic signatures of cirque components by the segmented objects in the different areas, which are the basis of subsequent object classification. For details on the parameter optimization used in this study Anders *et al.* (2011) are referred.

Because each cirque component has different segmentation parameters, all components need to be extracted separately. First objects are calculated in the entire area using the optimized segmentation parameters of the first component (step 6 in Figure 2) to create high-quality objects for one specific component. Subsequently, classification criteria were formulated based on expert knowledge (step 7 in Figure 2), and topographic signatures derived from the training samples served as inspiration and for determining threshold values of the classification criteria. Examples of classification criteria are "low NIR values" for cirque lake objects, "high relative elevation values" for cirque divide objects, and "high Slope Angle values" for cirque headwall objects. Manual heuristics are used to determine and fine-tune the threshold values of the classification criteria (steps 8 and 9 in Figure 2). After the classification rules are applied to the image objects, the cirque components are extracted (step 10 in Figure 2).

The remaining unclassified area is re-segmented with feature-specific segmentation criteria of the subsequent cirque component, and the procedure starts over from step 6 onwards, until all components are extracted (step 11 in Figure 2). As a consequence, the cirque components are extracted in a stratified fashion, where distinct and easy to identify components are extracted first (cirque lake and divide), and features with potential gradual or fuzzy boundaries last (cirque headwall and floor). Left-over objects are merged with neighboring classified objects when 100 percent enclosed by a single component, or labeled as "unclassified" so they are considered as not being part of the cirque complex. Classified objects were exported as Esri shapefiles for further analysis and visualization.

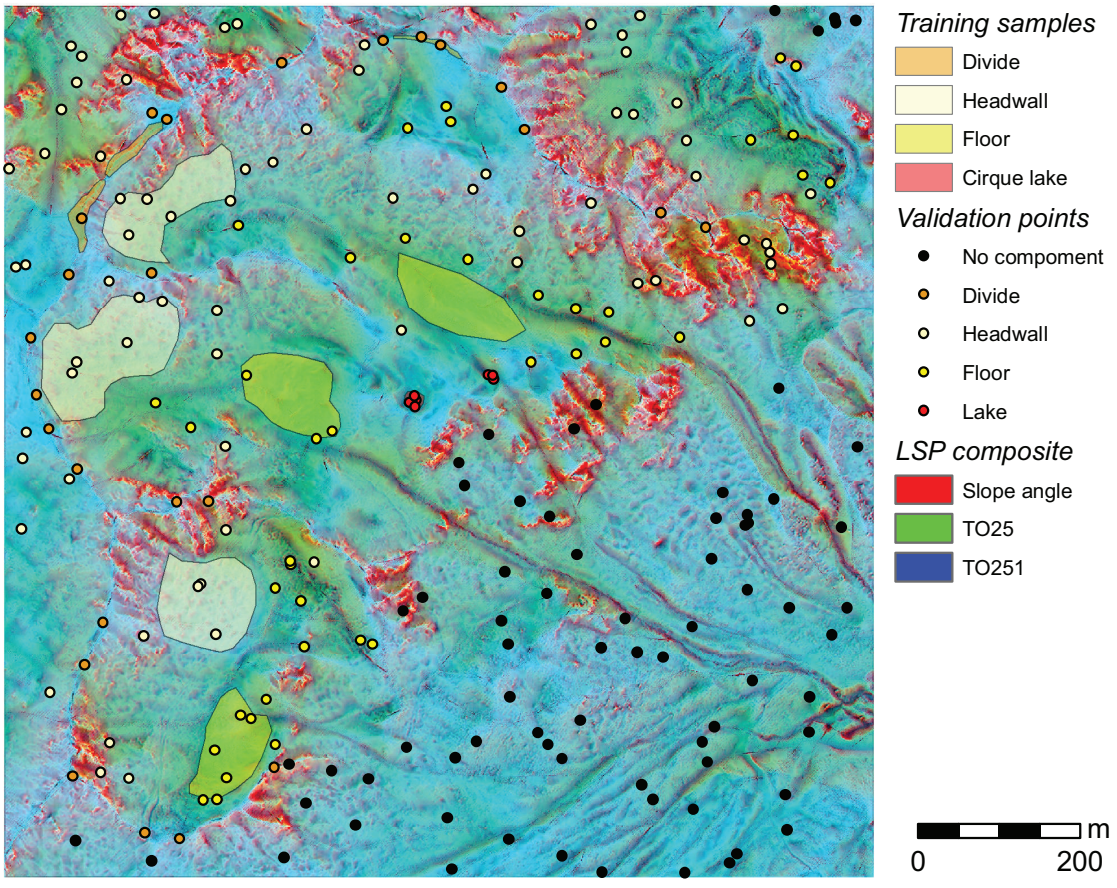

Plate 2. Training samples and validation points were manually digitized and labeled after interpretation of the CIR image and an LSP composite layer (with Slope Angle and Topographic Openness parameters (25 × 25 and 251 × 251 m search radius). The latter is shown in the background.

Table 2. Overview of the Optimal Segmentation Parameters

Component	Raster for segmentation	Scale parameter ∈ [1-inf]
Cirque lake	NIR	100
Divide	Slope & REL51	225
Floor	Slope & TO251	400
Headwall	Slope & TO251	400

Validation of the Rule Set

All classifications were evaluated systematically to determine the performance of the rule set in the different areas. In each area 200 random points were generated which were manually classified and labeled as Divide, Headwall, Floor, Lake, or "not part of a cirque." Where required, additional points were added so that all classes are sufficiently covered (i.e., at least 15 points).

The manual data set served as reference to validate the automated classification results. Here, point labels were compared with underlying classified polygons and as such a confusion matrix and derived user's accuracy, producer's accuracy, average accuracy, and KHAT statistic (Congalton, 1991) have been calculated. The classification scores served as measure to evaluate the performance of the classification rule set in each test area.

Results and Discussion

The Cirque Rule Set

The three main cirque components, and cirque lake are segmented based on the parameters presented in Table 2, and classified based on the criteria presented in Table 3. Cirque lakes are relatively small and divides are relatively narrow and are therefore segmented using relatively small scale parameters (respectively, 100 and 225). Elements of a cirque headwall and floor are generally larger and are therefore best outlined by larger objects, thus segmented using a larger scale parameter value (400).

The components are classified based on 13 individual rules, where cirque headwalls and floors are separated into core objects, which have a distinct morphological characterization, and surrounding objects. The surrounding objects may share characteristics of the core component, but show signs of disturbance or are in a transition towards another landform type or cirque component. When these neighboring objects border the core cirque component and share the topographic signature to a satisfying degree, they are also classified as such.

The rules have been summarized based on geomorphologically meaningful criteria. More specifically, cirque lakes are classified with low NIR values, due to the high absorption of near-infrared light by water. A second criterion is a low mean slope angle. Divides are commonly the highest landforms in the landscape, which was the motivation to formulate rules with relative elevation (measured over 51 × 51 meters and 251 × 251 meters). In addition, divides are normally not directly located next to cirque lakes which was formulated as a second rule, in order to prevent misclassifications of local maxima elsewhere in the area. Cirque floors can be characterized with relatively low slope angles, and are usually found within a certain distance from a cirque divide. Cirque headwalls are also found near divides, but have generally steeper slope angles than cirque floors.

Figure 3 presents the topographic signatures of the cirque components, based on the digitized training samples. The aforementioned descriptions can be recognized, and threshold values for the classification rules can be extracted. For example, divides are the only features with a mean relative elevation (over 251 × 251 meters) of more than 70 percent. Also, cirque headwalls and floors can be differentiated based on threshold slope angle value of 25 to 30 degrees in the training area. Cirque lakes generally have a mean slope angle of less than 10 degrees (including adjacent banks), and NIR values of less than 120 units. Figure 3 also shows that often the same criteria can be used to distinguish the different components, but that absolute threshold values are different between the areas. In area 2 and 3, cirque floors have generally steeper slope angles compared to floors in area 1 and 4.

Performance of the Rule Set

Plate 3 presents the classified objects in the four areas. Table 4 presents the accuracy metrics of the four areas. The rule set was trained based on Area 1, which also shows the highest average accuracy of 81 percent; 90 percent of the divides are correctly picked up, and 76 percent of the total (manually labeled) divides are classified, which are represented by the user's and producer's accuracies, respectively. Headwall and floor receive lower accuracy scores; they are more often confused with one another. While slope angle is the major criterion to differentiate both components, Figure 3 suggests that the topographic signatures of cirque headwalls and floors partly overlap and explains the confusion in the classification. All cirque lakes present in the area have been correctly classified.

Area 2 is located in a comparable altitudinal zone as Area 1, and so a comparable length of glacier occupation can be

Table 3. Overview of the Classification Rules

Rule nr	Component	Classifier	Data range	Value	Unit
1	Cirque lake	Mean NIR	0-255	< 100	DN
2		Mean slope	0-90	< 10	°
3	Divide	Distance to Cirque lake	0-inf	> 400	Pixels
4		Mean REL251	0-100	> 60	%
5		Mean REL51	0-100	> 60	%
6	Floor A (core)	Mean Slope	0-90	< 21	°
7		Distance to Divide	0-inf	< 900	Pixels
8	Floor B (surroundings)	Border to Floor A	YES/NO	YES	-
9		Mean slope	0-90	< 30	°
10	Headwall A (core)	Mean slope	0-90	> 29	°
11		Distance to Divide	0-inf	< 700	Pixels
12	Headwall B (surroundings)	Mean slope	0-90	> 29	°
13		Enclosed by Floor + Headwall	YES/NO	YES	-

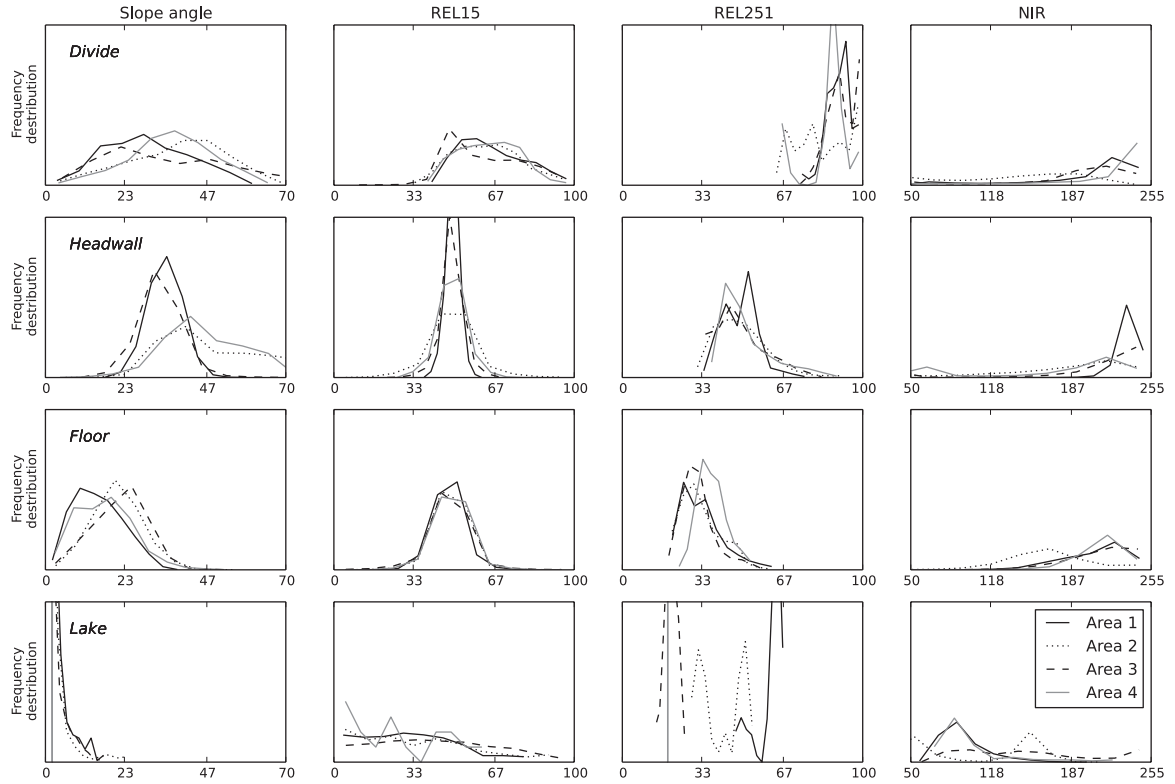

Figure 3. Topographic signatures of the cirque components in the different areas, on the basis of Slope Angle, Relative Elevation within 15 × 15 m and 251 × 251 m, and NIR values.

expected. Overall accuracy (71 percent) is acceptable and in agreement with Area 1. However, there are several noticeable differences. For example, only 59 percent of the labeled divides are classified, thus many divides are missed, which negatively influences the rest of the classification. Figure 3 shows lower values of relative elevation (within 251 × 251 m) which hints at the existence of wider divides, next to the narrow and sharp divides in Area 1. The widest divides are most likely missed and may explain the low producer's accuracy. In Area 2 floor and headwalls are also more often confused with each other than other components. All classified cirque lakes are correct, but a few are missed, likely due to higher NIR values in shallow water bodies (see also Figure 3).

Area 3 and 4 follow the same trend, but with decreasing accuracies due to further morphological deviation from the components of Area 1, particularly in Area 4 (the lowest test area) where only 29 percent of the classified cirque floor components are correct. Plate 3 shows the same trend where too great an area is incorrectly classified as cirque floor. In most cirques in the tested areas the cirque floor is separated from the main glacial valley bottom by a steeper slope, possibly part of the cirque threshold. This threshold is a hard boundary for the rule set to prevent classifying floor components. In Area 4, cirque thresholds are likely overlain by new sediments, have eroded away, or have never fully developed morphologically, which means that cirque floor components gradually merge with the main glacial valley without a threshold, resulting in glacial valley floors being misinterpreted as cirque floors by the rule set.

On the Transferability of Object-Based Rule Sets

This study focuses on the transferability of rule sets for the extraction of detailed and complex geomorphological features that contain information on their genetic history. Topographic signatures of the cirque components and the classification results indicate that when rule sets are adapted to local morphological conditions, higher classification accuracies can be achieved, and rule sets are transferable. This is in agreement with Rokitnicki-Wojcik *et al.* (2011), who mentioned that internally parameterized rule sets to map coastal marsh habitats performed only slightly better, in terms of classification accuracy, than rule sets that had been externally parameterized in nearby areas. Also Tiede *et al.* (2010) successfully applied a master rule set for the extraction of dwellings from satellite imagery data.

Yet, although our rule set was transferable to one other area, it was not producing accurate results in the other two test areas due to fundamental differences with the expression of landforms. In the following section, issues considering the transferability of the proposed rule set are addressed, followed by a discussion on the transferability of object-based rule sets in general.

First, cirque complexes in this study area have formed in locally different geological settings. When cirques form on initially steeper slopes, cirque headwall and floor components will show steeper slope signatures than in areas with a geological setting with initially more gentle hillslopes. Since slope angle was an important classifier to differentiate cirque headwall and floor, the boundary conditions are trained based on the local geological setting. To solve this, locally adapted boundary conditions can be introduced by using local training samples and may dramatically improve classification accuracy.

Second, the training areas are selected at different altitudinal zones, which introduces variation in the duration of glaciation, thus the degree to which glacial landforms have evolved, and the extent to which post-glacial landscape processes have modified the topographic signatures of "pure" glacial landforms. In other words, the topographic signatures of the cirque components contain different degrees of noise due to post-glacial landscape evolution.

Third, a stratified GEOBIA approach was applied where classifications of a second component were dependent on the classifications of a previous component. This means that classification error in an earlier step is transferred to a subsequent step to create even more error. For example, cirque divide are often

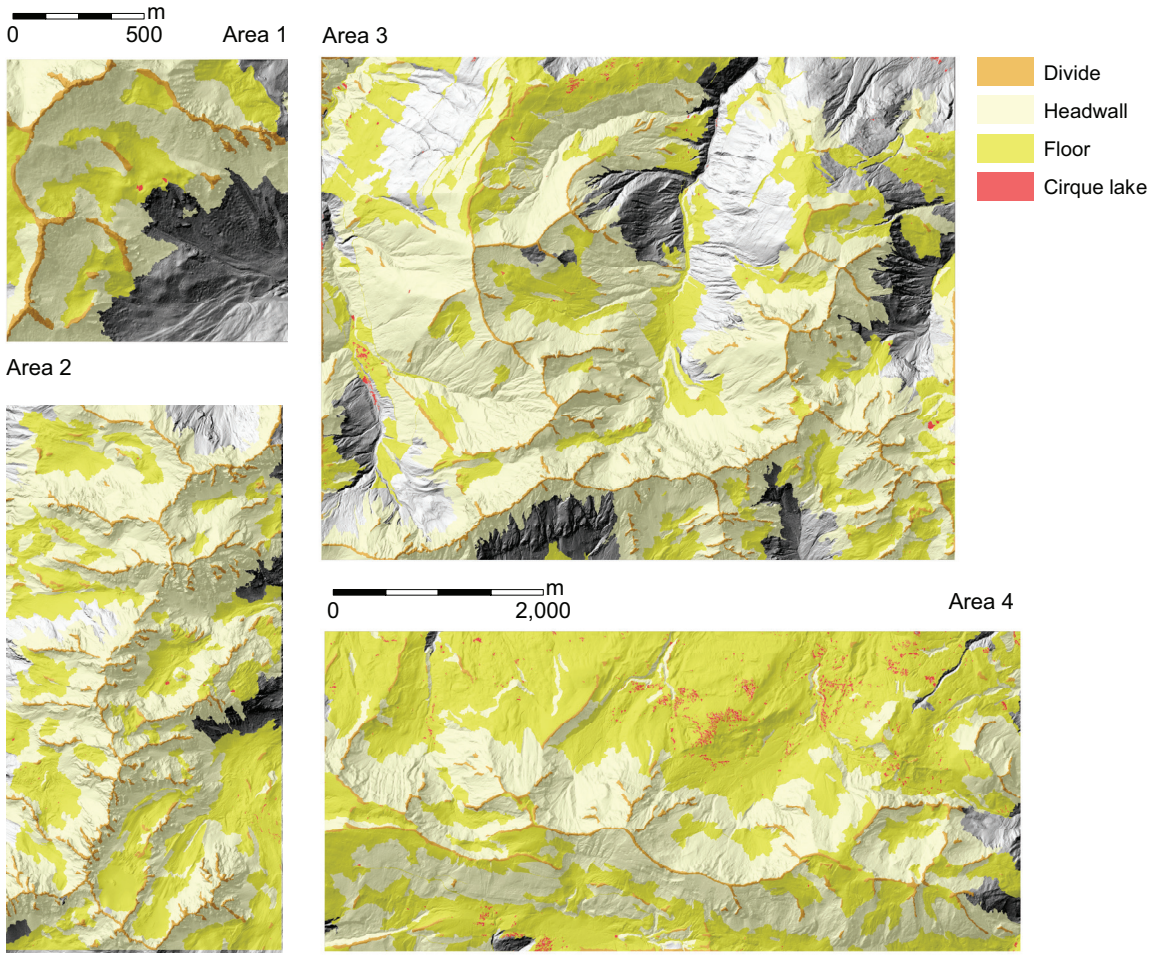

Plate 3. Final classification results showing the distribution of cirque components in the test areas. Object boundaries have been removed to increase the readability of the maps. Classification metrics are described in Table 4.

TABLE 4. OVERVIEW OF THE CLASSIFICATION ACCURACY METRICS

	User's accuracy [%]				Producer's accuracy [%]				Overall accuracy [%]	KHAT
	Divide	Headwall	Floor	Lake	Divide	Headwall	Floor	Lake		
Area 1	90	68	69	100	76	83	63	100	81	0.73
Area 2	84	72	60	100	59	92	70	63	71	0.58
Area 3	93	58	49	67	96	91	76	67	66	0.55
Area 4	86	78	29	0	71	69	89	0	51	0.33

classified correctly (high user's accuracy) but many (parts) of the divides are also missed by the classification (low producer's accuracy). Yet, cirque floor and headwall components are dependent on the existence of a cirque divide. This means that whenever the mean relative elevation values of cirque divides do not match the training signatures, for example when divides have evolved into more rounded or wider shapes than in the training area, a large portion of the classification fails.

In summary, the results suggest that to a certain extent, our rule set is transferable to nearby areas that share common geological and geomorphological history, if crucial classification thresholds are adapted to local topographic conditions. Yet, the rule set fails when geological differences, pre-glacial topography, or post-glacial geomorphological processes significantly changed or disguised topographic signatures of cirque components.

As a consequence, the rule set cannot be applied to, for example, the entire European Alps, to automatically map all cirque complexes. The question that arises is: "what is the largest area that can be analyzed with a single object-based rule set?" There is not a straightforward answer to this question, as it greatly depends on the diversity of the landscape, but should be considered when using Object-Based Image Analysis for landscape classifications.

Also, data sources and scale are important points of concern when it comes to transferability of rule sets. For example, the MR segmentation algorithm can work with multiple gridded data sets, with a different spatial resolution, at the same time. The scale parameter values are linked to the gridded data set with the smallest cell size, which is in this paper is 0.25 m for the CIR data set. This means that different scale parameter values are required if different resolution data is used, and as a result, parameter values cannot directly be compared with, or transferred to those from other studies which have used different resolution data. In addition, the value of LSPs is different when using different cell sizes. For example, Eisank *et al.* (2010) used curvature derived from a 10 m DTM as a basis for the extraction cirque divides. With 10 m grid cells, curvature is a meaningful parameter since the cirque divide is only one or few grid cells wide. In other words, the curvature is measured at the same scale as the

geomorphological feature of interest. In this research, elevation data with 1 m grid cells was used as main source. Applying rule sets of Eisank *et al*. (2010) on 1 m resolution data will not produce accurate results, as curvature is measured at a different scale (1 m) than the geomorphological feature of interest (10 m). This promotes an interesting discussion for future research on the optimal spatial resolution for specific geomorphological features, and applying multi-resolution data sets for whole landscape classifications.

In terms of the transferability of segmentation parameters, there is likely less concern, as long as objects are not too large and the data sets used have a similar standard deviation. Slightly under-segmented features compensate for potential segmentation errors (Dragut *et al*, 2014) as long as the same features in different areas are not too different from each other in terms of size and shape (Anders, 2013).

Expert knowledge remains a crucial step in the design of the rule set and the assessment of the transferability to other areas. We therefore encourage experts from different geoscientific disciplines to translate detailed field knowledge into arithmetic or relational concepts, which in turn can be translated as classification rules. In that way, common patterns can be used to optimize existing classification rules or designing more generic rules for the classification of true morphogenetic features.

Conclusions

The focus of this paper was to create and test the transferability of an object-based rule set for the semi-automated extraction of cirque components in Vorarlberg using airborne lidar data and CIR imagery. The rule set successfully extracted cirque divides, cirque headwalls, cirque floors, and the subcomponent cirque lake with an overall accuracy of 81 percent in the training area. In addition, the presented rule set was transferable to nearby areas that shared a common geological and geomorphological history if crucial classification thresholds were adapted to local topographic conditions. However, this failed when geological differences, pre-glacial topography or post-glacial geomorphological processes significantly changed or disguised topographic signatures of cirque components. These findings hinder straightforward upscaling by application of rule sets to larger research areas. Expert knowledge remains a crucial step in the design of the rule set, size of the study area, and assessment of the transferability to other areas.

Acknowledgments

This project was partly funded by Interreg Project Smart Inspectors (Project number: *I-1-03=176*). In addition, financial support was provided by the Virtual Lab for e-Science (vl-e) project and internal funds of the Computational Geo-Ecology department of the University of Amsterdam. We are grateful to the "Land Vorarlberg" (*www.vorarlberg.at*) in Austria for free use of the lidar data. Robin Gabriner is thanked for his work on cirque extraction. Mike Smith is thanked for providing useful comments to the manuscript.

References

Anders, N.S., A.C. Seijmonsbergen, and W. Bouten, 2011. Segmentation optimization and stratified object-based analysis for semi-automated geomorphological mapping, *Remote Sensing of Environment*, 115(12):2976-2985.

Anders, N.S., 2013. *Modeling Alpine Geomorphology Using Laser Altimetry data*, Ph.D. dissertation. University of Amsterdam, The Netherlands, 143 p.

Anders, N.S., A.C. Seijmonsbergen, and W. Bouten, 2013. Geomorphological change detection using object-based feature extraction from multi-temporal LiDAR data, *IEEE Geoscience and Remote Sensing Letters*, 10(6):1587-1591.

Ardelean, F., M. Török-Oance, P. Urdea, and A. Onaca, 2011. Application of object based image analysis for glacial cirques detection, Case study: The Ţarcu Mountains (Southern Carpathians). *Forum Geographic*, 10(1):20-26.

Baatz, M., and A. Schäpe, 2000. Multiresolution Segmentation - An optimization approach for high quality multi-scale image segmentation, *Angewandte Geographische Informationsverarbeitung* XII (J. Strobl, T. Blaschke, and G. Griesebner, editors), Wichmann, Heidelberg, pp. 12-23.

Belgiu, M., and L. Drăguţ, 2014. Comparing supervised and unsupervised multiresolution segmentation approaches for extracting buildings from very high resolution imagery, *Journal of Photogrammetry and Remote Sensing*, 96:67-75.

Congalton, R.G., 1991. A review of assessing the accuracy of classifications of remotely sensed data, *Remote Sensing of Environment*, 37(1):35-46. Drăguţ, L., and T. Blaschke, 2006. Automated classification of landform elements using object-based image analysis, *Geomorphology*, 81(3-4):330–344.

Drăguţ, L., O. Csillik, C. Eisank, and D. Tiede, 2014. Automated parameterisation for multi-scale image segmentation on multiple layers. *Journal of Photogrammetry and Remote Sensing*, 88: 119–127

Drăguţ, L., and T. Blaschke, 2006. Automated classification of landform elements using object-based image analysis. *Geomorphology*, 81(3-4): 330–344.

Eisank, C., L. Drăguţ, J. Götz, and T. Blaschke, 2010. Developing a semantic model of glacial landforms for object-based terrain classification-the example of glacial cirques, *Proceedings of GEOBIA 2010 - Geographic Object-Based Image Analysis* (E.A. Addink, and F.M.B. Coillie, editors), Ghent University, Ghent, Belgium, 29 June - 02 July, ISPRS, Vol. XXXVIII-4/C7.

Eisank, C., 2013. *An Object-Based Workflow for Integrating Spatial Scale and Semantics to Derive Landforms from Digital Elevation Models*, Ph.D. dissertation, Interfakultärer Fachbereich für Geoinformatik-Z_GIS, Salzburg, Austria, 142 p.

Evans, I.S., 2012. Geomorphometry and landform mapping: What is a landform?, *Geomorphology* 137(1):94-106.

Graaff, L.W.S. de, M.G.G. De Jong, and A.C. Seijmonsbergen, 2007. Landwirtschaft-entwicklung und Quartär, *Geologie der Österreichischer Bundesländer Vorarlberg* (J.G. Friebe, editor), Verlag Geologische Bundesanstalt, Vienna, Austria, pp. 21-32.

Ivy-Ochs, S., H. Kerschner, A. Reuther, F. Preusser, K. Heine, M. Maisch, P.W. Kubik, and C. Schlüchter, 2008. Chronology of the last glacial cycle in the European Alps, *Journal of Quaternary Science*, 23(6-7):559-573.

Rokitnicki-Wojcik, D., A. Wei, and P. Chow-Fraser, 2011. Transferability of object-based rule sets for mapping coastal high marsh habitat among different regions in Georgian Bay, Canada, *Wetlands Ecology and Management*, 19: 223-236

Saha, K., N.A. Wells, and M. Munro-Stasiuk, 2011. An object-oriented approach to automated landform mapping: A case study of drumlins, *Computers and Geosciences*, 37(9):1324-1336.

Smith, M.J., and C.F. Pain, 2009. Applications of remote sensing in geomorphology, *Progress in Physical Geography*, 33(4):568-582.

Smith, M.J., J. Rose, and S. Booth, 2006. Geomorphological mapping of glacial landforms from remotely sensed data: An evaluation of the principal data sources and an assessment of their quality, *Geomorphology*, 76(1-2):148-165.

Schneevoigt, N.J.,S. Van der Linden, H. Thamm, and L. Schrott, 2008. Detecting Alpine landforms from remotely sensed imagery, A pilot study in the Bavarian Alps, *Geomorphology*, 93(1-2):104-119.

Tiede, D., S. Lang, D. Hölbling, and P. Füreder, 2010. Transferability of OBIA rulesets for IDP camp analysis in Darfur, *Proceedings of GEOBIA 2010 - Geographic Object-Based Image Analysis* (E.A. Addink and F.M.B. Coillie, editors), Ghent University, Ghent, Belgium, 29 June-02 July, ISPRS, Vol. No. XXXVIII-4/C7.

Yokoyama, R., M. Shirasawa, and R.J. Pike, 2002. Visualizing topography by openness: a new application of image processing to digital elevation models, *Photogrammetric Engineering and Remote Sensing*, 68(3): 257–265

Zhang, Y. J., 1996. A survey on evaluation methods for image segmentation, *Pattern Recognition*, 29(8):1335-1346.